Heavy Mo isotope enrichment in the Pitcairn plume: implications for the subduction cycle of anoxic sediments

Qasid Ahmad, Martin Wille, Jabrane Labidi, Stephan König, Colin Devey, Klaus Mezger

Heavy Mo isotope enrichment in the Pitcairn plume: implications for the subduction cycle of anoxic sediments

Qasid Ahmad[1*], Martin Wille[1], Jabrane Labidi[2], Stephan König[3], Colin Devey[4], Klaus Mezger[1,5]

[1]Institut für Geologie, Universität Bern, Baltzerstrasse 1+3, 3012 Bern, Switzerland

[2]Université de Paris Cité, Institut de Physique du Globe de Paris, CNRS, 75005 Paris, France

[3]Instituto Andaluz de Ciencias de la Tierra (IACT), CSIC & UGR, Avenida de las Palmeras 4, Armilla, 18100 Granada, Spain

[4] GEOMAR, Helmholtz Centre for Ocean Research, 24148 Kiel, Germany

[5]Center for Space and Habitability, Universität Bern, Gesellschaftsstrasse 6, 3012 Bern, Switzerland

**Corresponding author: qasid.ahmad@univ-lorraine.fr*

Present address: Université de Lorraine - Centre de Recherches Pétrographiques et Géochimiques (CRPG), UMR7358 CNRS, 54500 Vandoeuvre-les-Nancy, France

Keywords: molybdenum isotopes, enriched mantle, Pitcairn Island, LLSVP, anoxic sediment, recycling, subduction zones

Abstract

Subduction redistributes elements between Earth's principal geochemical reservoirs, modifying the chemical composition of Earth's mantle, crust, atmosphere, and hydrosphere, and consequently having an impact on the evolution of life itself. Subduction of surface material that has been geochemically modified by low-temperature processes leads to mineralogical and chemical heterogeneities in mantle reservoirs over time and is recorded in modern ocean island basalts. One of the principal geochemical end members of the heterogeneous deep mantle, the enriched mantle 1 (EM-1) source of Pitcairn Island, has been attributed to the contribution of crustal material with vastly different chemical compositions and ages. The Mo isotope composition of lavas from Pitcairn Island constrains the nature of this recycled crustal component. Pitcairn lavas have elevated $\delta^{98/95}$Mo relative to the depleted mantle. The high $\delta^{98/95}$Mo is associated with high time-integrated ^{232}Th/^{238}U and ^{87}Rb/^{86}Sr, and low time-integrated ^{147}Sm/^{144}Nd and ^{238}U/^{204}Pb. These characteristics can be attributed to the recycling of nearly pristine pelagic sediments that were deposited in a Proterozoic anoxic deep-ocean into the sources of the Pitcairn Island lavas. The isotope composition of these lavas is similar to that of EM-1 hotspots from the South Atlantic, indicating the addition of reduced sediments in both of Earth's large low shear wave velocity provinces (LLSVPs). Consistent data from both locations imply that the subduction cycling of sedimentary redox-sensitive elements such as Mo, S, Se, and U into arc magmas was in these cases inefficient in the Precambrian and the chemical and isotopic signature of reduced sediments is preserved in the source of ocean island basalts bearing the EM-1 characteristics.

Introduction

Plate tectonics and Earth's surface oxygenation are intimately linked and influence the Earth's principal geochemical reservoirs by redistributing elements over time (e.g., Kump and Barley, 2007; Campbell and Allen, 2008; Keller and Schoene, 2012; Lee et al., 2016; Smit and Mezger, 2017). Chemical fractionation processes during subduction determine the composition of Earth's mantle, crust, atmosphere, and hydrosphere, and consequently have an impact on the distribution of elements

essential for life (Zerkle, 2018). The subduction of material which has been geochemically modified by near-surface, low-temperature processes leads to distinct chemical heterogeneities in Earth's interior. Melts derived from such heterogeneities can provide complementary information about secular changes in the surface redox conditions (e.g., Cabral et al., 2013; Andersen et al., 2015; Gaschnig et al., 2017, 2021b; Stolper and Bucholz, 2019; Liu et al., 2019; Dottin et al., 2020; Yierpan et al., 2020; Ahmad et al., 2022). The variation in the isotope composition of redox-sensitive stable metal isotopes in plume-influenced mid-ocean ridge basalts (MORB) and ocean island basalts (OIB) can be used to further constrain the origin, nature, and scale of compositional heterogeneity in the Earth's deep mantle, which has conventionally been constrained by major- and trace-element, and radiogenic isotope systematics.

The elemental and isotope signatures of Mo are distinct between the mantle and surface reservoirs due to the incompatible behavior of Mo during magmatic processes (e.g., Newsom et al., 1986) and its redox-dependent aqueous mobility and mass-dependent fractionation (e.g., Bali et al., 2012; Freymuth et al., 2015; König et al., 2016; Kendall et al., 2017; Chen et al., 2019; Villalobos-Orchard et al., 2020; Ahmad et al., 2021). Therefore, Mo isotopes can track the subduction of variously redox-affected, surface-derived material into the mantle (e.g., Gaschnig et al., 2021b; Ma et al., 2022; Ahmad et al., 2022; Hin et al., 2022). The Mo isotope systematics are particularly suitable to study element transfer among different surface and mantle reservoirs because the extent of Mo isotope fractionation during prograde subduction metamorphism depends on the Mo mobility (e.g., Chen et al., 2019; Ahmad et al., 2021, 2022), which in turn depends on the oxygen fugacity (fO_2) in the associated subduction zone fluids (Bali et al., 2012; Skora et al., 2017; Chowdhury et al., 2022). Thus, the stable Mo isotope ratio of a subducted slab integrates the redox-dependent aqueous mobility of Mo during subduction processes (Ahmad et al., 2022).

From a global perspective, the redox state of subducting sediments is a reflection of Earth's surface O_2 budget (e.g., Evans, 2012). This leads to distinct Mo elemental abundances and isotopic

compositions of arc magmas depending on the redox conditions of the respective subducted sediments (Freymuth et al., 2016; Gaschnig et al., 2017; Ahmad et al., 2021). This surface signature can also modify deep mantle domains and is recorded in melts derived from plumes that sample these domains (Gaschnig et al., 2021b; Ahmad et al., 2022). These melts that potentially carry a recycled oceanic sediment component in turn can provide insights into redox conditions during ancient sediment deposition, which is known to have changed over Earth's history from dominantly anoxic to oxic conditions, and subsequent sediment subduction (Ahmad et al., 2022). While oxic sediments are expected to have low Mo concentrations and low $\delta^{98/95}$Mo (down to -1.5 ‰) due to prominent loss of isotopically heavy Mo^{6+} during early subduction (Ahmad et al., 2021), anoxic sediments preserve pre-subduction Mo isotope signatures and elemental abundances due to the immobile behavior of Mo in anoxic subduction settings (Ahmad et al., 2022). Due to the prevailing anoxic deep-ocean conditions during the Precambrian, the lower Mo mobility and availability, the small/non-existent oxic sink (i.e. Fe-Mn oxide-rich sediments enriched in light Mo), Precambrian deep-ocean anoxic sediments are expected to have Mo isotope compositions and elemental abundances similar to the upper continental crust (UCC; $\delta^{98/95}$Mo ≈ +0.05 to 0.15 ‰; Willbold and Elliot, 2017 and references therein), while Phanerezoic anoxic sediments exhibit higher enrichments of heavy Mo (e.g., Kendall et al., 2017; Gaschnig et al., 2021b; Ahmad et al., 2022). Therefore, the Mo concentration and isotope composition of the subducted sediment layer indirectly records the oxidation state of the Earth's surface (Ahmad et al., 2022). This study provides constraints on the origin and genesis of the Pitcairn mantle source using variations of the stable isotopes of Mo in basalts collected from active submarine volcanoes about 80 km east of the island of Pitcairn in the South-Pacific Ocean during the Polynaut cruise (1999) (Hekinian et al., 2003).

Pitcairn Island represents one of the end member type-localities of the compositionally heterogeneous deep mantle, the enriched mantle 1 (EM-1) domain, and is associated with the Pacific large low shear wave velocity province (LLSVPs) (e.g., French and Romanowicz, 2015; Jackson et al., 2021). Pitcairn

Island basalts have close to primordial Ne isotope ratios (Honda and Woodhead, 2005) associated with highly radiogenic $^{87}Sr/^{86}Sr$ and $^{208}Pb/^{204}Pb$, and some of the least radiogenic $^{206}Pb/^{204}Pb$ among known OIBs (Woodhead and Devey, 1993). This enriched component requires a low time-integrated μ ($^{238}U/^{204}Pb$) associated with high time-integrated κ ($^{232}Th/^{238}U$) and $^{87}Rb/^{86}Sr$. Different recycled geochemical reservoirs have been proposed to explain the enriched mantle source of Pitcairn Island, including metasomatized lithospheric mantle, pelagic sediments, marine carbonates, and lower continental crust (e.g., Woodhead and McCulloch, 1989; Eisele et al., 2002; Stracke, 2012; Garapić et al., 2015; Delavault et al., 2016; Wang et al., 2018; Labidi et al., 2022). The age of potentially recycled subducted sediments was interpreted to be Precambrian based on radiogenic isotopes and stable S isotopes (Eisele et al., 2002; Garapić et al., 2015; Delavault et al., 2016; Labidi et al., 2022). The occurrence of a sediment component in the source of the Pitcairn basalts can be tested using Mo isotopes. Due to the redox-sensitive behavior of Mo, recycled anoxic (Precambrian) deep-sea sediments will exhibit a Mo isotope composition that is heavier than the depleted mantle (Ahmad et al., 2022). Previously analyzed samples from Pitcairn Island include only subaerial lavas. They display $\delta^{98/95}Mo$ lower than the depleted mantle (Gaschnig et al., 2021b). The light isotopic signature, however, was explained by the influence of tropical weathering due to the correlation with Mo/Ce ratios and a secular disequilibrium recorded by $^{238}U/^{234}U$ ratios (Gaschnig et al., 2021b). Therefore, it was not possible to constrain the primary Mo isotope signature of the Pitcairn mantle plume. The active seamounts studied here offer fresh basaltic glassy material that is likely not affected by secondary alteration after the eruption and thus can be expected to preserve the geochemical characteristics of the hotspot. In order to ensure that the chemical signature of the volcanic material is primary, only glassy rims of pillow basalts were analyzed. The material was collected with the Nautile submersible from the flanks of the seamounts “Bounty” and “Volcano 5”. All samples are well-characterized in terms of radiogenic isotopes (Sr, Nd, and Pb), S isotopes, volatile abundances, and major element abundances (Labidi et al., 2022). Furthermore, selected trace element data are available (Clog, 2010) making this

material ideal to study the EM-1 end member component of the Pitcairn mantle source with Mo isotopes.

Analytical methods

Molybdenum purification and isotope analyses were conducted in the clean laboratory facilities at the Institute of Geological Sciences, University of Bern. Enough sample powder was weighed into pre-cleaned Savillex™ Teflon® vials to obtain 100 to 500 ng Mo for each analysis. The samples were spiked with an enriched isotope tracer solution (^{97}Mo-^{100}Mo double spike) prior to dissolution. The samples were dissolved in concentrated single-distilled HF-HNO_3 (1.5 mL:0.5 mL mixture) at 100°C for at least 24 h. To surpress fluoride formation, additional 0.5 mL of concentrated HNO_3 was added to the sample during evaporation. The dry residue was then re-dissolved in 6 M HCl and evaporated after being heated for at least 24 h. To dissolve all precipitated fluorides, this step was conducted three times, with increasing heating temperature during each of these steps in the order: (i) 100 °C, (ii) 120 °C, (iii) 140 °C.

The dissolved samples were processed through anion- and cation exchange columns to obtain a clean Mo separate (Wille et al., 2013). In the first step, samples were taken up in 3 ml 4 M HCl + 0.15% H_2O_2 and passed through 1.5 ml Dowex 1X8, 200-400 mesh, anion resin (ca. 10 mm column width). Additional 4 ml of the loading acid and 2 ml of 18.2 MΩ·cm deionized water were used to elute most matrix elements except for Fe, which was subsequently eluted with 6 ml 3 M HNO_3 together with Mo. In a second step, the sample material was taken up in 2 ml of 0.5 M HCl + 0.10% H_2O_2 and passed through 2 ml Dowex 50WX8 200-400 mesh cation exchange resin (ca. 10 mm column width) to separate Fe. Additional 5 ml of the loading acid were used to recover Mo quantitatively. Measurement of stable Mo isotopes were carried out on a Neptune Plus MC-ICP-MS coupled with an Aridus II desolvating nebulizer with an uptake rate of 100 µl·min^{-1} (details are provided in Ahmad et al., 2021). Six Mo isotopes (^{94}Mo, ^{95}Mo, ^{96}Mo, ^{97}Mo, ^{98}Mo, and ^{100}Mo) were measured simultaneously as well as ^{99}Ru and ^{101}Ru to monitor potential isobaric interferences. All isotopes were measured with 10^{-11} Ω

resistors with the exception of ^{101}Ru, which was measured using a 10^{-12} Ω resistor. A combination of 'H' Ni sampler cone and 'H' Ni skimmer cone for analyses provided a signal intensity of ~ 45 V/ppm on ^{95}Mo. A double spike correction method based on an iterative calculation procedure (see Siebert et al., 2001) was used to obtain the natural isotope ratios of the sample. The total procedural blank was 0.71 to 0.74 ng, which is less than 1 % of the total analyzed Mo. Mo isotope compositions are presented in the δ-notation relative to NIST SRM 3134 in ‰ (Greber et al., 2012; Goldberg et al., 2013) with an interference correction based on ^{99}Ru:

$$\delta^{98/95}\mathrm{Mo} = \left(\frac{\left(\frac{^{98}\mathrm{Mo}}{^{95}\mathrm{Mo}}\right)_{\mathrm{Sample}}}{\left(\frac{^{98}\mathrm{Mo}}{^{95}\mathrm{Mo}}\right)_{\mathrm{NIST\ SRM\ 3134}}} - 1 \right) * 1{,}000$$

$\delta^{98/95}$Mo values corrected for Ru interferences using ^{99}Ru and ^{101}Ru were compared to ensure accurate correction for Ru interference on Mo ($\Delta^{98/95}\mathrm{Mo}_{^{99}\mathrm{Ru}-^{101}\mathrm{Ru}}$ < 0.01 ‰). To correct for background Mo, sample measurements were bracketed by measurements of a 0.5 M HNO_3 carrier solution on-peak. Molybdenum isotope signals in the background solution were 10^4 times smaller than during the sample measurement. Sample and background analyses consisted of 80 and 10 cycles, respectively, with a signal integration time of 4.194 s for each cycle. Repeated measurements of the standard NIST SRM 3134 and an in-house J&M standard solution (JMCBern) lot 602332B gave an isotopic difference of $\Delta^{98/95}$Mo = 0.260 ± 0.023 ‰ (2 SD, n = 10), in agreement with other studies (Greber et al., 2012; Ahmad et al., 2021, 2022; Kaufmann et al., 2021; O'Sullivan et al., 2021). Solution standards were measured at a concentration of 50 ppb. Chemically purified whole-rock reference materials AGV-2 and BHVO-2 yielded a $\delta^{98/95}$Mo of −0.175 ± 0.037 ‰ (2 SD, n = 3) and −0.077 ± 0.024 ‰ (2 SD, n = 3) (Table S-1). The values are within uncertainty of those determined previously (e.g., Burkhardt et al., 2014; Willbold et al., 2016; Zhao et al., 2016). Individual measurements of whole rock reference

materials (Table S-1) are within the long-term 2SD external reproducibility of ± 0.05 ‰ as determined by previous measurements of BHVO-2 (Ahmad et al., 2021, 2022).

Including previous BHVO-2 measurements (−0.09 ± 0.05 ‰; n = 11), we consider ± 0.05 ‰ as the long-term 2 SD external reproducibility of the sample measurements. All samples and whole-rock reference materials were measured multiple times (after one single digestion and chemical separation) and the obtained $\delta^{98/95}$Mo values were averaged for data presentation and interpretation (Table S-1). All individual sample measurements differ less than ± 0.05 ‰ from their average $\delta^{98/95}$Mo.

Results

The $\delta^{98/95}$Mo values of Pitcairn basaltic glass samples exhibit a small range between −0.12 ‰ and −0.09 ‰ (n=10), with an average of −0.11 ‰ (Table 1; Fig. 1, 2). The variations among Pitcairn basalts are smaller than the external 2SD reproducibility of ± 0.05 ‰ (Table 1). Within analytical uncertainty, all samples are isotopically heavier than the depleted mantle ($\delta^{98/95}$Mo ≈ −0.20 ‰; Bezard et al., 2016; McCoy-West et al., 2019; Hin et al., 2022). These results differ from previously published Mo isotope data of Pitcairn Island lavas that were measured on material that was influenced by subaerial weathering (Gaschnig et al., 2021b). Overall, Mo concentrations range between 1.26 and 4.40 µg/g and are higher than average MORB (log mean = $\sim 0.38^{+0.95}_{-0.27}$ µg/g, 2SD; Gale et al., 2013). Only considering the least differentiated samples, with MgO content ranging from 4.6 to 5.6 wt%, a large [Mo] variability from 1.26 to 2.93 µg/g is observed. Furthermore, Mo/Ce ratios are variable (0.022 to 0.038) overlapping with average MORB Mo/Ce (~0.035 ± 0.02, 2SD; Gale et al., 2013) (Fig. 2). The samples have $^{87}Sr/^{86}Sr$, $^{143}Nd/^{144}Nd$, $^{206}Pb/^{204}Pb$, and $^{208}Pb/^{204}Pb$ isotope ratios that are characteristic of the EM-1 mantle reservoir (Labidi et al., 2022). The radiogenic isotope signatures of the basalts are similar to the most enriched EM-1 influenced MORBs from the South-Mid Atlantic Ridge (Fig. 3).

Table 1. *Mo concentration and isotope data for Pitcairn Island lavas. Literature data from Labidi et al. (2022), except (A) (Bourdon and Van Orman, 2009). La/Sm and Ce concentrations are available for selected samples (Clog, 2010). Element oxides are in wt%, minor and trace elements are in µg/g.*

sample ID	pn03-01	pn03-02	pn03-03	pn03-05	pn03-07	pn03-08	pn03-10	pn03-11	pn08-07	pn14-04
seamount	Bounty	Bounty	Bounty	Bounty	Bounty	Bounty	Bounty	Bounty	Volcano 5	Bounty
depth (mbsl)	2508	2508	2500	2408	2276	2250	2165	1957		1705
Na_2O	4.2	4.2	4.2	3.8	3.9	4.2	3.5	4.0	4.2	4.2
SiO_2	47.8	47.9	47.7	47.8	47.6	48.8	50.6	48.9	54.4	54.2
K_2O	1.4	1.4	1.5	1.4	1.4	1.6	0.8	1.6	2.7	2.3
Al_2O_3	16.0	16.0	15.8	15.4	15.3	16.2	15.1	15.3	16.1	15.3
CaO	9.1	9.1	9.1	9.8	9.7	8.1	8.6	8.7	4.9	5.4
MgO	5.4	5.5	4.8	5.2	5.4	5.0	5.6	4.6	2.6	2.6
P_2O_5	0.7	0.7	0.8	0.7	0.7	0.8	0.5	0.8	1.2	1.2
FeO	9.7	9.8	9.7	9.9	10.0	9.7	9.6	9.7	9.1	9.5
MnO	0.2	0.2	0.2	0.2	0.2	0.2	0.1	0.2	0.2	0.2
TiO_2	2.9	2.9	3.0	3.1	3.1	3.3	3.1	3.4	1.9	2.2
total	97.5	97.6	96.8	97.2	97.1	97.9	97.6	97.2	97.2	97.0
Mo	2.47	1.26	2.45	2.23	1.53	2.93	1.38	2.41	4.40	4.22
Cl	502	494	498	426	424	459	324	417	493	750
Cu	59	50	52	50	56	33	37	50	3	11
H_2O	9192	9807	9662	8512	8125	9099	5696	5667		12123
S^{2-}	1279	1299	1133	953	875	738	1017	569	602	507
Ce				70.4	69.7	77.0	48.9	69.9		
K_2O/TiO_2	0.49	0.48	0.49	0.44	0.45	0.49	0.27	0.47	1.40	1.06
CaO/Al_2O_3	0.57	0.57	0.58	0.63	0.63	0.50	0.57	0.57	0.30	0.36
Cl/K	0.04	0.04	0.04	0.04	0.04	0.03	0.05	0.03	0.02	0.04
S^{2-}/S_{tot}	0.97	0.98	0.80	0.95	0.91	1.00	0.95	0.72	1.00	0.99
Mo/Ce				0.032	0.022	0.038	0.028	0.034		
$(La/Sm)_N$				2.66	2.64	3.17	2.07	3.17		
$\delta^{98/95}$Mo (‰)	−0.121	−0.121	−0.112	−0.113	−0.111	−0.119	−0.115	−0.111	−0.097	−0.093
δ^{34}S (‰)	0.1	0.2	−1.0	−1.2	−1.3	−1.0	−1.2	−1.2	1.6	0.7
Δ^{33}S (‰)	0.020	0.028	0.025	0.028	0.012	0.027	0.030	0.031	0.026	0.007
Δ^{36}S (‰)	0.08	0.08	0.05	0.13	0.08	0.06	0.06	0.06	0.02	−0.06
$^{206}Pb/^{204}Pb$	17.742	17.742	17.749	17.816	17.809	17.747	17.926	17.770		18.198
$^{207}Pb/^{204}Pb$	15.470	15.470	15.474	15.482	15.479	15.475	15.493	15.479		15.516
$^{208}Pb/^{204}Pb$	38.569	38.570	38.579	38.645	38.658	38.644	38.798	38.668		38.916
$^{143}Nd/^{144}Nd$			0.512567	0.512599	0.512583	0.512537		0.512944		0.512762
$^{87}Sr/^{86}Sr$	0.704483	0.704477	0.704485	0.704482	0.704498	0.704624	0.704481	0.704531		0.704002
$^{87}Sr/^{86}Sr^A$				0.70446		0.70463	0.70447		0.70530	

Discussion

The Pitcairn lavas define the end member of the EM-1 component. Their composition is a result of a complex history of mixing processes prior to eruption, including mantle source enrichment, low degrees of partial mantle melting, followed by magmatic differentiation and sulfide segregation, and variable extents of volatile loss via degassing (e.g., Woodhead and McCulloch, 1989; Eisele et al., 2002; Garapić et al., 2015; Delavault et al., 2016; Wang et al., 2018; Labidi et al., 2022). All these processes can potentially affect the Mo isotopic composition of the erupted melts.

The potential effect of secondary and magmatic processes on $\delta^{98/95}$Mo

The primary isotope composition of Mo preserved in rocks and minerals can be modified by direct or indirect interaction with seawater. Although careful separation of fresh glass avoids the former, it is not possible to detect visually magmatic assimilation of altered oceanic crust (AOC) that happened en route to the surface or to eliminate all traces of Fe-Mn coating in picked samples. The Cl/K ratios are < 0.05 for Bounty lavas and <0.02 for Volcano 5 samples (Labidi et al., 2022) (Table 1), which is below the threshold of 0.10, above which lavas are considered to be contaminated significantly by Cl-rich brines (Michael and Cornell, 1998). These low Cl/K ratios exclude Cl enrichment by assimilation of hydrated oceanic crust, interaction with brine, and seawater alteration. Furthermore, seawater alteration should affect the sample $^{87}Sr/^{86}Sr$, while $^{143}Nd/^{144}Nd$ remains unchanged (e.g.,Labidi et al., 2013), which is not observed in subaerial Pitcairn lavas (not shown; Garapić et al., 2015). Isotope effects caused by Mo adsorped on Fe-Mn oxides can be excluded as well, because this would have shifted the Mo isotope composition towards $\delta^{98/95}$Mo<depleted mantle ($\delta^{98/95}$Mo ≈ –0.20 ‰; Bezard et al., 2016; McCoy-West et al., 2019; Hin et al., 2022). It is also unlikely that seafloor alteration, oceanic crust assimilation, or Mn-oxide contribution would generate a statistically homogeneous $\delta^{98/95}$Mo in all investigated samples derived from different sampling depths (Table 1).

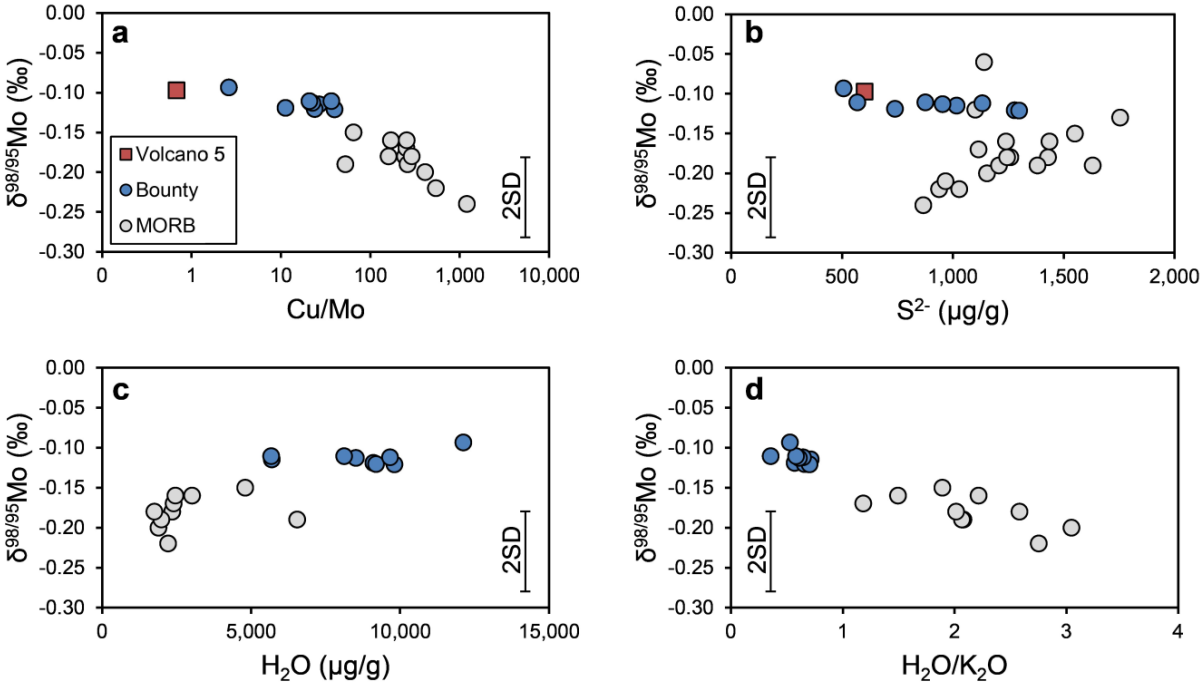

Figure 1. *Plots of $\delta^{98/95}$Mo vs. (a) Cu/Mo; (b) S^{2-}; (c) H_2O; (d) H_2O/K_2O. Error bars indicate 2 SD external reproducibility. MORB data is from the literature (Clog et al., 2013; Labidi et al., 2014; Bezard et al., 2016). Three isotopically heavy outliers from Bezard et al. (2016) are excluded.*

The variability of the bulk S contents in Pitcairn lavas is attributed to continuous tholeiite-like sulfide segregation and magmatic degassing (Labidi et al., 2022) that may have also affected the Mo isotope composition of the residual silicate melt (e.g., Greber et al., 2014; Liang et al., 2017; Kaufmann et al., 2021; Hin et al., 2022). Increasing sulfide melt segregation, indicated by decreasing Cu/Mo ratios in the silicate melt, due to the more chalcophile affinity of Cu does not show any covariation with $\delta^{98/95}$Mo while previously reported MORB display an overall trend (Fig. 1). Furthermore, no control of magmatic degassing on the Mo isotope composition is observed, because the variable H_2O (and H_2O/K_2O) and S contents of the basaltic glass samples, which correlate with water depth (Labidi et al., 2022), are decoupled from Mo isotopes (Fig. 1).

No measurable isotopic difference among the least and most primitive samples (i.e. pn03-10 and pn14-04; Fig. 2, Fig S-1) is observed indicating that the effect of fractional crystallization (e.g., Voegelin et al., 2014; Wille et al., 2018) is negligible on the Mo isotope composition of the Pitcairn samples. This

observation has been made in other magmatic systems (e.g., Yang et al., 2015; Bezard et al., 2016; Nebel-Jacobsen et al., 2021; Gaschnig et al., 2021a).

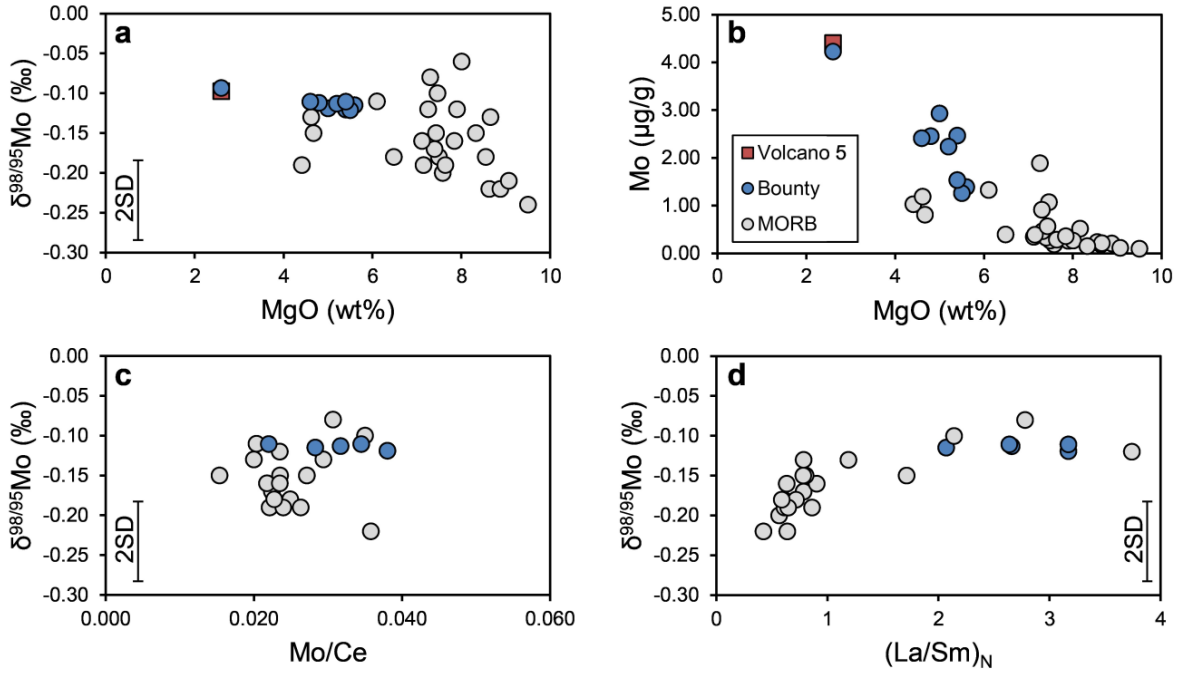

Figure 2. *Plots of (a) $\delta^{98/95}$Mo vs. MgO; (b) Mo vs. MgO; (c) $\delta^{98/95}$Mo vs. Mo/Ce; (d) $\delta^{98/95}$Mo vs. $(La/Sm)_N$. Error bars indicate 2 SD external reproducibility. MORB data is from Bezard et al. (2016). Three isotopically heavy outliers from Bezard et al. (2016) are excluded.*

The Mo/Ce and La/Sm ratios vary significantly in the samples from Pitcairn Island (Fig 2), potentially indicating different extents of low-degree partial melting of their source. Low-degree melting would result in high $\delta^{98/95}$Mo (McCoy-West et al., 2019; Chen et al., 2022), due to the presence of both, Mo^{6+} and Mo^{4+} in the mantle, and associated higher incompatibility of isotopically heavy Mo^{6+} over light Mo^{4+} during mantle melting. The homogeneous $\delta^{98/95}$Mo values of the basaltic lavas indicate that low-degree mantle melting had an insignificant effect on the Mo isotope composition of investigated lavas. This indicates a minor influence of low-degree melts on the Mo isotope composition of plume-influenced OIBs compared to MORB settings (e.g., East Pacific Rise; Chen et al., 2022). This can be explained by melting at higher temperatures along the hotter plume-adiabat (e.g., Putirka, 2008; Ahmad et al., 2022) or by Mo being present in only one oxidation state ($Mo^{6+}/\Sigma Mo = 1$), resulting in negligible effects on Mo isotope fractionation during mantle melting.

The potential role of recycled components

As the heavy Mo isotope composition of Pitcairn Island basalts cannot be attributed to assimilation or mineral fractionation, the enrichment of the EM-1 component in ^{98}Mo is most likely a mantle source feature. Various recycled plate materials have been proposed to contribute to EM-1 plume sources, including metasomatized lithospheric mantle, oceanic sediments, and components from the lower continental crust (e.g., Woodhead and McCulloch, 1989; Eisele et al., 2002; Stracke, 2012; Garapić et al., 2015; Delavault et al., 2016; Wang et al., 2018; Labidi et al., 2022).

Processes involving fluid-driven enrichments of isotopically heavy Mo in the subcontinental mantle in convergent plate settings (e.g., Freymuth et al., 2015; König et al., 2016; Chen et al., 2019; Ahmad et al., 2021) could in principle account for the data. A similar model was proposed to explain the O isotope data of Pitcairn Island phenocrysts (Eiler et al., 1995). However, systematic enrichments or depletions of fluid mobile elements are not observed in the Pitcairn Island source (Willbold and Stracke, 2006), in line with Mo/Ce ratios not significantly exceeding MORB values (e.g., Freymuth et al., 2015; König et al., 2016; Villalobos-Orchard et al., 2020). Recycled lower continental crust (LCC) material has been suggested to be a major component of the Pitcairn Island mantle source (e.g., Stracke, 2012 and references therein). There is no estimate of $\delta^{98/95}$Mo of the LCC. Cumulates that possibly reside in the LCC, however, likely have light Mo isotope signatures (Wille et al., 2018; Nebel-Jacobsen et al., 2021) and are unsuitable candidates to explain the observed Mo isotope compositions in the basalt samples. Isotopically heavy arc-derived cumulates that can be explained by slab-derived fluid contamination (Storck et al., 2023), are not in line with fluid mobile element systematics, as discussed above.

Furthermore, the low time-integrated ^{238}U/^{204}Pb, which is characteristic of the Pitcairn EM-1 mantle source, and overall unradiogenic ^{206}Pb/^{204}Pb indicate that recycled isotopically variable altered oceanic crust (Freymuth et al., 2015; Ahmad et al., 2021) cannot produce the EM-1 characteristics. Phanerozoic subducted sediments and mafic oceanic crust are isotopically light (Chen et al., 2019; Ahmad et al.,

2021) and can also not contribute to the isotopically heavy composition of the EM-1 component. Previous studies have attributed the radiogenic isotope and stable Mg isotope composition of the Pitcairn Island mantle source to the recycling of (Precambrian) subducted marine carbonates (Delavault et al., 2016; Wang et al., 2018). The recycling of carbonate components has likely an undetectable effect on the Mo isotope ratio of an enriched mantle component due to the low distribution of dissolved Mo during authigenic carbonate formation leading to low Mo concentrations (<< 100 ng/g) in pure carbonate (e.g., Voegelin et al., 2009, 2010; Thoby et al., 2019). Furthermore, Precambrian seawater contained even less dissolved Mo (e.g., Anbar, 2008) that could be extracted by carbonate formation. Therefore, depending on marine deposition conditions, the Mo signature in carbonate successions is often dominated by clastic and organic phases.

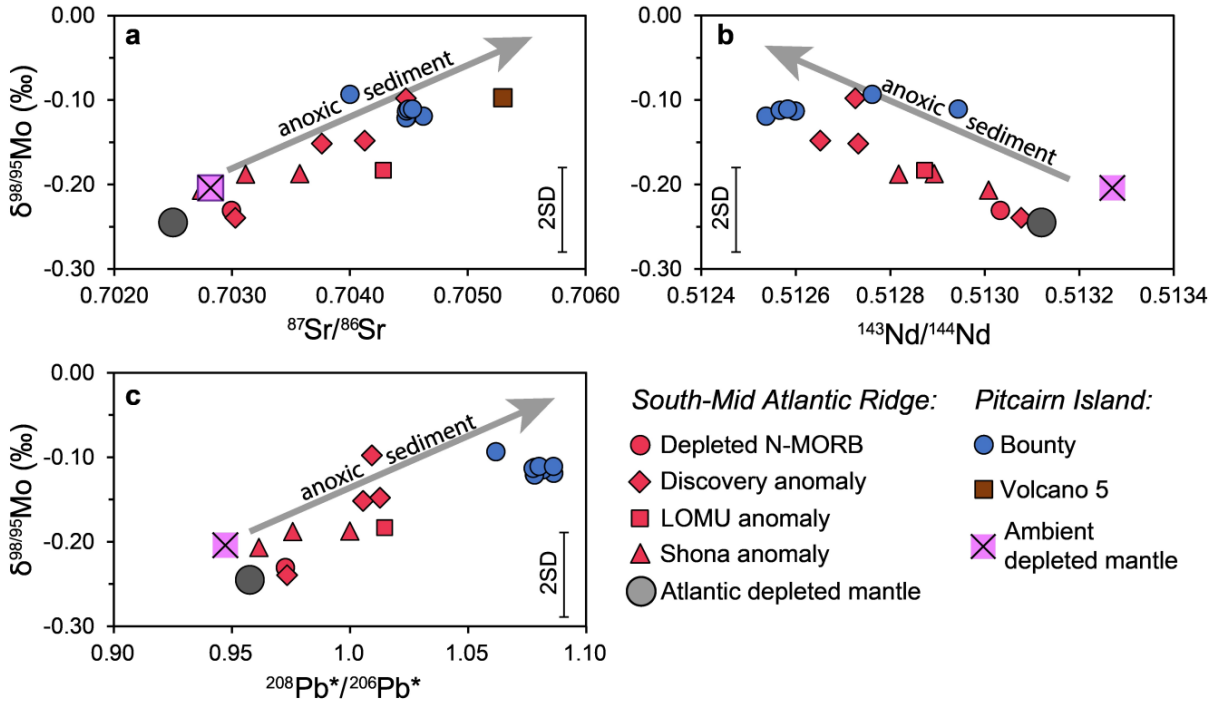

Figure 3. *Covariation diagram of EM-1 influenced lavas from South-Mid Atlantic Ridge (Douglass et al., 1999; Ahmad et al., 2022) and Pitcairn Island (this study). (a) $\delta^{98/95}$Mo vs. $^{87}Sr/^{86}Sr$; (b) $\delta^{98/95}$Mo vs. $^{143}Nd/^{144}Nd$; $\delta^{98/95}$Mo vs. $^{208}Pb^*/^{206}Pb^*$ (time-integrated Th/U). Error bars indicate 2 SD external reproducibility. Values for Atlantic and ambient depleted mantle are in Table S-2.*

When compared with radiogenic isotopes and other EM-1 mantle plume influenced lavas from the South-Mid Atlantic Ridge (S-MAR), a general trend towards an enriched mantle source is evident

(Fig. 3). This covariation was previously interpreted as a result of the recycling of Mid-Proterozoic anoxic deep-ocean sediments into the mantle source (Ahmad et al., 2022). To infer the hypothetical sediment end member, a misfit model (Supplementary Information) using Sr isotope and elemental systematics of the ambient mantle and a model Mid-Protoerozoic sediment was applied. This is necessary to visualize different mixing lines/hyperbolas due to various potential combinations of [Mo] and $\delta^{98/95}$Mo in the sediment end member. The misfit model suggests that a Precambrian pelagic sediment contributed to the observed Mo isotope systematics (Fig. 4).

Different ages for the recycled sediments in the mantle source of Pitcairn Island lavas have been proposed. Labidi et al. (2022) argued that based on the small range of Δ^{33}S and Δ^{36}S (Table 1) most likely Proterozoic (reduced) sediments were recycled into the mantle source of Pitcairn Island. The Proterozoic ocean was redox-stratified (e.g., Canfield, 1998) with oxygenated shallow waters and higher organic matter (OM) input closer to the continents, while the deep-sea remained anoxic with lower input of OM (e.g., Lyons et al., 2014; Laakso and Schrag, 2019). The literature data of Proterozoic OM-rich sediments (Fig. 4; Table S-2) represent mostly shallow-marine (continental shelf/closed basins) sediments from anoxic/euxinic settings, where e.g., sulfate reduction leads to higher authigenic accumulation of isotopically variable Mo from seawater compared to lower Mo accumulation in the anoxic deep-sea. In these deep waters, the Mo isotope signature and concentration of the sedimentary end member is expected to be close to UCC (Fig. 4; Ahmad et al., 2022). The best fit of the sedimentary end member of the Pitcairn mantle source (blue curve in Fig. 4) is located in the lower 1 SD (lower than 4.10 µg/g) of the compiled Proterozoic OM-rich sediment data (Supplementary Information) close to the UCC composition. This suggests that the Pitcairn mantle source is contaminated by Proterozoic deep-ocean sediments with limited heavy Mo isotope enrichment. An addition of less than 2 % of this sedimentary material is needed to account for the heavy Mo signature of the Pitcairn Island mantle source (2 component mixing between UCC and DM; Table S-2). Although mantle-like O isotope signatures within basalt phenocrysts have been used to argue against

a sedimentary origin for the EM-1 source of Pitcairn Island (Eiler et al., 1995, 1997), a sediment contribution below ~2% remains undetected with stable O isotopes (Eiler et al., 1995). In addition, modeling of a sedimentary end member based on S-isotope as well as radiogenic isotope data of the Pitcairn samples (Table 1; Table S-2) (Labidi et al., 2022), suggests that a contribution of ≤ 2% anoxic Proterozoic deep-sea sediments can fulfill the trace element and isotope systematics of the EM-1 source of Pitcairn Island. Due to the increased compatibility of Mo^{4+} in stable Mo-bearing hosts such as rutile or sulfides (see Bali et al., 2012; Skora et al., 2017; Chowdhury et al., 2022) in the anoxic subducted sedimentary units, it is expected that Mo is immobile in reduced sediments during prograde subduction metamorphism. Therefore, no significant isotope fractionation during the subduction of reduced sediment is expected. Thus, the original sedimentary Mo isotope signatures and element abundances are preserved in the deep mantle (Ahmad et al., 2022). Such behavior is not expected for Mo in Phanerozoic oxidized sediments because of the prominent loss of heavy Mo^{6+} during (early) prograde subduction metamorphism (Ahmad et al., 2021).

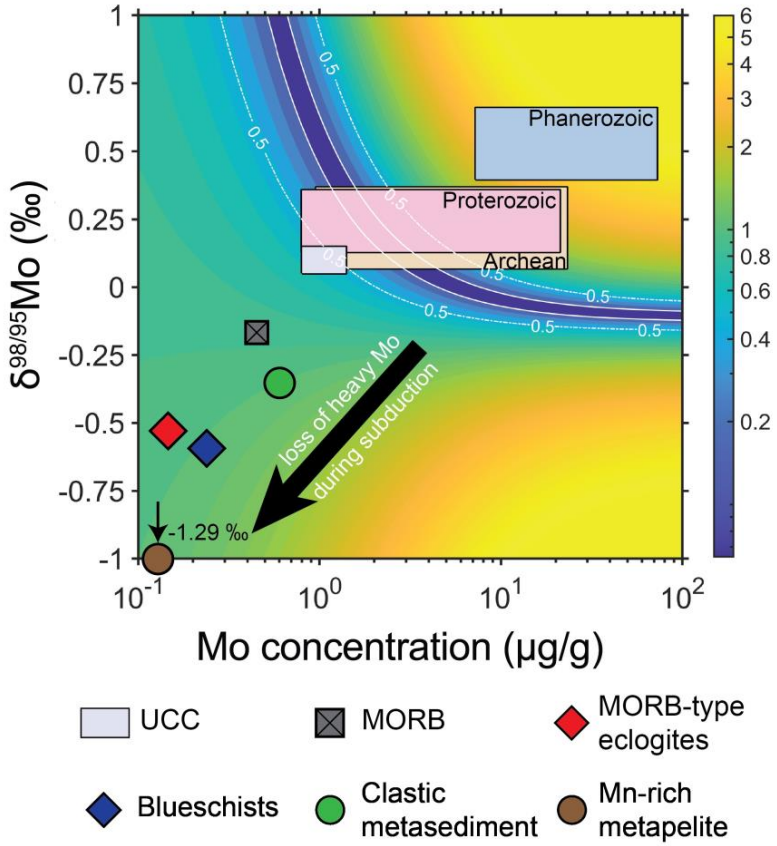

Figure 4. *Least squares error ($\Delta^{98/95}$Mo in ‰; up to 6 ‰) between calculated mixing lines and analyzed samples (after Ahmad et al., 2022). The best fit is indicated by the blue field. Variables are the $\delta^{98/95}$Mo and [Mo] values derived from the $\delta^{98/95}$Mo vs. $^{87}Sr/^{86}Sr$ relationship (Fig. 3). Literature values for potential (concentration averaged) recycled lithologies, and anoxic sediments sorted by age intervals are shown for comparison. See Supplementary Information for references, mixing parameters, and further details.*

Anoxic pelagic sediments as a source for EM-1

The contribution of (Mid-)Proterozoic sediments to the source of the Pitcairn hotspot is supported by other studies (e.g., Woodhead and McCulloch, 1989; Eisele et al., 2002; Delavault et al., 2015). A (Mid-)Proterozoic pelagic sediment end member has also been identified for EM-1 influenced lavas from the S-MAR that interact with the Discovery- and Shona mantle plumes, based on correlations between radiogenic isotopes of Sr, Nd, and Hf, and fO_2-sensitive stable isotope variations of S, Se, and Mo (Douglass et al., 1999; Andres et al., 2002; le Roux et al., 2002; Labidi et al., 2013; Yierpan et al., 2020; Ahmad et al., 2022) (Fig 3). The Mo and radiogenic isotope systematics of the Pitcairn lavas are

similar to S-MAR (Fig. 3). A cross-plot of $\delta^{98/95}$Mo vs. $^{87}Sr/^{86}Sr$, $^{143}Nd/^{144}Nd$, and $^{208}Pb^*/^{206}Pb^*$ (time-integrated Th/U) shows that the Pitcairn lavas influenced by the EM-1 component extend the covariation recorded in S-MAR samples, pointing towards a similar Proterozoic pelagic sedimentary end member with a Mo isotopic composition heavier than the depleted mantle (Fig. 3). It is likely that Proterozoic deep-ocean processes under anoxic conditions also controlled the Th/U ratios of the sedimentary end member producing the EM-1 Pb-isotope signatures in Pitcairn Island and S-MAR lavas (Fig 3c). Under reducing conditions, U is immobile and shows a geochemical behavior very similar to Th. However, Th is much more particle-reactive than U, independently of ocean redox conditions, leading to higher Th enrichments over U in deep-sea pelagic sediments similar to present-day pelagic clays (Plank and Langmuir, 1998). The chemical composition of modern pelagic sediments differs from those deposited in Precambrian anoxic deep waters, because potential U hosts such as biogenic phosphate (bone and teeth debris) and Fe-Mn oxides were absent. The absence of these U hosts together with a much lower concentration of dissolved U in the ocean reservoir (Lyons et al., 2014) lowered the U flux into deep-sea sediments. The redox-stratified Proterozoic ocean instead probably favored significant U accumulation in organic matter (OM)-rich settings close to the continents (e.g., Lyons et al., 2014; Laakso and Schrag, 2019). Therefore, it can be argued that the EM-1 source signature reflects the contamination by pelagic sediments with elevated Th/U, low U/Pb, and high $\delta^{98/95}$Mo from a continental source with enrichments of particle-reactive Th and Pb from a Mo- and U-depleted Proterozoic redox-stratified ocean. Furthermore, deep-mantle contamination with anoxic material is supported by C isotope data of CO_2 degassed at Pitcairn Island and other OIBs. These C isotope data are consistent with recycled reduced C in the mantle source of the lavas (Eguchi et al., 2020). The sequestration of reduced sediments into the deep mantle can also have enabled the oxygenation of Earth's surface (Duncan and Dasgupta, 2017).

The global occurrence of anoxic deep-ocean bottom waters over most of the Proterozoic (e.g., Lyons et al., 2014) together with the low abundances of passive margins during the formation and

stabilization of the Columbia supercontinent during the Mid-Proterozoic (e.g., Bradley, 2011) probably provided the potential for widespread accumulation of anoxic pelagic sediments with potentially high $\delta^{98/95}$Mo and Th/U. The fact that two EM-1 influenced suites (i.e. Pitcairn and Shona/Discovery plumes) from two different LLSVPs, i.e. the Pacific and the African, show an input with a common radiogenic and Mo isotope composition (Fig. 3) suggests widespread recycling of (Mid-) Proterozoic anoxic pelagic sediments into the deep mantle, most likely at the subduction girdle surrounding the supercontinent (see Li et al., 2019). This is further supported by the geologic record, where Precambrian deep-ocean sediments are generally absent due to subduction of the oceanic crust (Patchett et al., 1984; Sperling et al., 2015).

Hin et al. (2022) suggested that the subchondritic $\delta^{98/95}$Mo observed for the upper mantle (-0.20 ± 0.01 ‰) is the result of the continuous recycling of an isotopically light subduction-modified oceanic crust. In their model, the subduction of different proportions of oceanic crust and sediment on different time scales (1.1 to 3.9 Gyr) can explain the isotopically light composition of the upper mantle or the mantle as a whole. Our findings show that mixing of the upper mantle with oceanic crust and sediments would have opposing effects on the Mo isotopic signature of a mantle source, as subducted Precambrian sediments are expected to possess a heavy UCC-like isotopic signature, while the subducted oceanic crust has possibly a light isotope composition (Chen et al., 2019; Ahmad et al., 2021). Furthermore, the widespread accumulation of Precambrian sediments in the LLSVPs suggests that a significant proportion of crustal material is not recycled back to the bulk (or upper) mantle by convective stirring. The higher density of the underlying subducted oceanic crust favored large scale deposition of ancient subducted oceanic crust in the LLSVPs (Jones et al., 2020; Niu, 2018; Wang et al., 2020) preventing its effective mixing into the bulk mantle. Therefore, there are contrasting effects of prograde subduction metamorphism on the sediment elemental and isotope signature depending on the prevailing redox state of the ocean (Ahmad et al., 2021, 2022) and an inefficient homogenization of the mantle. This is not an argument against a subducted crustal component in the upper mantle,

however, but this suggests that the calculated recycling time scales and volumes may need to be refined.

Implications for subduction cycling of redox-sensitive elements

These findings support the model that the redox structure of Earth's surface is directly connected to the deep-mantle compositional differences in $\delta^{98/95}$Mo (Gaschnig et al., 2021b), which in turn inform about redox conditions of subducted material (Ahmad et al., 2022). Phanerozoic subducted Mn-Fe rich sediments can efficiently buffer subduction zone fluids towards oxidizing conditions (see Ague et al., 2022). On the other hand, subducted anoxic sediments, which were abundant in the Precambrian, buffer redox conditions during prograde subduction metamorphism to reduced conditions (Ahmad et al., 2022; Padron-Navarta et al., 2023). The widespread subduction of anoxic material and the preservation of isotopic signatures of Mo, Se, and S characteristic of sediments in EM-1 sources (Labidi et al., 2013; Yierpan et al., 2020; Ahmad et al., 2022) suggests a stable sulfide (and possibly rutile) phase during the related Precambrian subduction and negligible mobilization of these elements during prograde subduction metamorphism. As a consequence, decreased subduction recycling efficiency into the mantle wedge and ultimately arc magmatism is expected for these (and probably other) redox-sensitive elements during the Proterozoic compared to the times of dominant oxidized sediment subduction in the Phanerozoic. This is supported by Mo elemental and isotope systematics from the Lesser Antilles Arc suggesting a limited transfer of anoxic sediment-derived Mo to the mantle wedge (Freymuth et al., 2016; Gaschnig et al., 2017). Other redox-sensitive element systematics suggest inefficient subduction recycling of e.g., U during the Precambrian except during the major oxidation events (Liu et al., 2019) and limited redox transfer to the mantle wedge as indicated by Fe^{3+}/Fe^{2+} and V/Sc ratios in arc lavas, which systematically rose only after the Neoproterozoic Oxidation Event when oxidation made sulfates in the deep-ocean available for subduction (Stolper and Bucholz, 2019). This further supports the notion that subducted anoxic sediments act as a redox filter that could buffer fluids from the underlying AOC and serpentinites to reducing conditions independent

of their original fO_2 (Padron-Navarta et al., 2023). This low fO_2 consequently leads to suppressed redox budget transfer into arc magmas as well as mobility of e.g., Mo, Se, S, and U. This potentially results in changing abundances of these elements in continent-forming magmatic rocks over deep time, depending on the redox budget of subducted lithologies, which in turn is related to Earth's surface oxygenation.

Conclusion

The lavas from Pitcairn Island define the known end member of the EM-1 mantle component. This makes them particularly suitable to constrain the chemical and isotopic composition of this distinct and important mantle component and elucidate its genesis. Applying mixing models using combined Mo and radiogenic isotopes from fresh Pitcairn hotspot basalts suggests that <2% of Proterozoic pelagic sediments formed near the anoxic base of a stratified ocean are a plausible contaminant to explain the Mo isotopic signature of the Pitcairn mantle source. This conclusion is in line with EM-1 influenced lavas from the South Atlantic, where a recycled anoxic sediment contribution was proposed previously (Ahmad et al., 2022). Radiogenic isotopes and stable Mo isotopes from both settings suggest a common origin of the widespread contamination of Earth's LLSVPs, likely caused by the subduction of Proterozoic anoxic pelagic sediments. These findings complement those of Hin et al. (2022), who inferred predominantly light Mo isotope signatures recycled to the (bulk) mantle by adding anoxic Precambrian sediments. The addition of this anoxic and isotopically heavy material to the core-mantle boundary, which is not largely recycled back to the bulk mantle by convective stirring, may therefore be critical in refined models of silicate Earth evolution driven by subduction recycling through time. This further confirms that the Mo isotope signature of enriched hotspot lavas with a recycled sedimentary component can constrain the redox state before and during the subduction of those. The preservation of pre-subducted sedimentary Mo and S isotope signatures in the EM-1 mantle source suggests decreased subduction recycling of redox-sensitive elements like Mo, Se, S, and U from

these sediments into the mantle wedge during the Precambrian. In addition, it supports the interpretation that the EM-1 component of the mantle includes ancient surface material.

Acknowledgements

This study was funded by the Swiss National Science Foundation, Switzerland (Grant number 182508) to MW. The MC-ICP-MS at the Institute of Geological Sciences, University of Bern used in this study was acquired within the framework of the NCCR project PlanetS (Grant nr. 1NF40-141881) funded by the Swiss National Science Foundation. SK acknowledges Ramón y Cajal fellowship RYC2020-030014-I and grant PID2021-122793NB-I00. Nick Greber is acknowledged for discussions that contributed to this manuscript. We thank the two anonymous reviewers for constructive comments that helped to improve the paper. Rosemary Hickey-Vargas is thanked for editorial handling.

References

Ague, J.J., Tassara, S., Holycross, M.E., Li, J.-L., Cottrell, E., Schwarzenbach, E.M., Fassoulas, C., and John, T., 2022, Slab-derived devolatilization fluids oxidized by subducted metasedimentary rocks: Nature Geoscience 2022, p. 1–7, https://doi.org/10.1038/s41561-022-00904-7.

Ahmad, Q., Wille, M., König, S., Rosca, C., Hensel, A., Pettke, T., and Hermann, J., 2021, The Molybdenum isotope subduction recycling conundrum: A case study from the Tongan subduction zone, Western Alps and Alpine Corsica: Chemical Geology, v. 576, p. 120231, https://doi.org/10.1016/J.CHEMGEO.2021.120231.

Ahmad, Q., Wille, M., Rosca, C., Labidi, J., Schmid, T., Mezger, K., and König, S., 2022, Molybdenum isotopes in plume-influenced MORBs reveal recycling of ancient anoxic sediments: Geochemical Perspectives Letters, v. 23, p. 43–48, https://doi.org/10.7185/GEOCHEMLET.2236.

Anbar, A.D., 2008. Elements and Evolution. Science v. 322, p. 1481–1483. https://doi.org/10.1126/science.1163100

Andersen, M.B., Elliott, T., Freymuth, H., Sims, K.W.W., Niu, Y., and Kelley, K.A., 2015, The terrestrial uranium isotope cycle: Nature 2015 517:7534, v. 517, p. 356–359, https://doi.org/10.1038/nature14062.

Andres, M., Blichert-Toft, J., and Schilling, J.-G., 2002, Hafnium isotopes in basalts from the southern Mid-Atlantic Ridge from 40°S to 55°S: Discovery and Shona plume–ridge interactions and the role of recycled sediments: Geochemistry, Geophysics, Geosystems, v. 3, p. 1–25, https://doi.org/10.1029/2002GC000324.

Bali, E., Keppler, H., and Audetat, A., 2012, The mobility of W and Mo in subduction zone fluids and the Mo-W-Th-U systematics of island arc magmas: Earth and Planetary Science Letters, v. 351–352, p. 195–207, https://doi.org/10.1016/j.epsl.2012.07.032.

Bezard, R., Fischer-Gödde, M., Hamelin, C., Brennecka, G.A., and Kleine, T., 2016, The effects of magmatic processes and crustal recycling on the molybdenum stable isotopic composition of

Mid-Ocean Ridge Basalts: Earth and Planetary Science Letters, v. 453, p. 171–181, https://doi.org/10.1016/j.epsl.2016.07.056.

Bourdon, B., & Van Orman, J. A. 2009, Melting of enriched mantle beneath Pitcairn seamounts: Unusual U–Th–Ra systematics provide insights into melt extraction processes. Earth and Planetary Science Letters, 277(3-4), p. 474-481. https://doi.org/10.1016/j.epsl.2008.11.017.

Bradley, D.C., 2011, Secular trends in the geologic record and the supercontinent cycle: Earth-Science Reviews, v. 108, p. 16–33, https://doi.org/10.1016/j.earscirev.2011.05.003.

Cabral, R.A., Jackson, M.G., Rose-Koga, E.F., Koga, K.T., Whitehouse, M.J., Antonelli, M.A., Farquhar, J., Day, J.M.D., and Hauri, E.H., 2013, Anomalous sulphur isotopes in plume lavas reveal deep mantle storage of Archaean crust: Nature, v. 496, p. 490–493, https://doi.org/10.1038/nature12020.

Campbell, I.H., and Allen, C.M., 2008, Formation of supercontinents linked to increases in atmospheric oxygen: Nature Geoscience, v. 1, p. 554–558, https://doi.org/10.1038/ngeo259.

Canfield, D.E., 1998. A new model for Proterozoic ocean chemistry. Nature v. 396, p. 450–453. https://doi.org/10.1038/24839.

Chen, S., Hin, R.C., John, T., Brooker, R., Bryan, B., Niu, Y., and Elliott, T., 2019, Molybdenum systematics of subducted crust record reactive fluid flow from underlying slab serpentine dehydration: Nature Communications, v. 10, https://doi.org/10.1038/s41467-019-12696-3.

Chen, S., Sun, P., Niu, Y., Guo, P., Elliott, T., and Hin, R.C., 2022, Molybdenum isotope systematics of lavas from the East Pacific Rise: Constraints on the source of enriched mid-ocean ridge basalt: Earth and Planetary Science Letters, v. 578, p. 117283, https://doi.org/10.1016/J.EPSL.2021.117283.

Chowdhury, P., Dasgupta, R., Phelps, P.R., Costin, G., and Lee, C.T.A., 2022, Oxygen fugacity range of subducting crust inferred from fractionation of trace elements during fluid-present slab melting in the presence of anhydrite versus sulfide: Geochimica et Cosmochimica Acta, v. 325, p. 214–231, https://doi.org/10.1016/J.GCA.2022.02.030.

Clog, M., 2010, Concentration et composition isotopique en hydrogène du manteau terrestre. PhD thesis - Institut de Physique du Globe de Paris, Paris, France.

Clog, M., Aubaud, C., Cartigny, P., Dosso, L., 2013. The hydrogen isotopic composition and water content of southern Pacific MORB: A reassessment of the D/H ratio of the depleted mantle reservoir. Earth and Planetary Science Letters v. 381, p. 156–165. https://doi.org/10.1016/j.epsl.2013.08.043.

Delavault, H., Chauvel, C., Sobolev, A., and Batanova, V., 2015, Combined petrological, geochemical and isotopic modeling of a plume source: Example of Gambier Island, Pitcairn chain: Earth and Planetary Science Letters, v. 426, p. 23–35, https://doi.org/10.1016/j.epsl.2015.06.013.

Delavault, H., Chauvel, C., Thomassot, E., Devey, C.W., and Dazas, B., 2016, Sulfur and lead isotopic evidence of relic Archean sediments in the Pitcairn mantle plume: Proceedings of the National Academy of Sciences of the United States of America, v. 113, p. 12952–12956, https://doi.org/10.1073/pnas.1523805113.

Dottin, J.W., Labidi, J., Lekic, V., Jackson, M.G., and Farquhar, J., 2020, Sulfur isotope characterization of primordial and recycled sources feeding the Samoan mantle plume: Earth and Planetary Science Letters, v. 534, p. 116073, https://doi.org/10.1016/J.EPSL.2020.116073.

Douglass, J., Schilling, J.-G., and Fontignie, D., 1999, Plume-ridge interactions of the Discovery and Shona mantle plumes with the southern Mid-Atlantic Ridge (40°-55°S): Journal of Geophysical Research: Solid Earth, v. 104, p. 2941–2962, https://doi.org/10.1029/98JB02642.

Duncan, M.S., Dasgupta, R., 2017. Rise of Earth's atmospheric oxygen controlled by efficient subduction of organic carbon. Nature Geoscience v. 10, p. 387–392. https://doi.org/10.1038/ngeo2939

Eguchi, J., Seales, J., and Dasgupta, R., 2020, Great Oxidation and Lomagundi events linked by deep cycling and enhanced degassing of carbon: Nature Geoscience, v. 13, p. 71–76, https://doi.org/10.1038/s41561-019-0492-6.

Eiler, J.M., Farley, K.A., Valley, J.W., Hauri, E., Craig, H., Hart, S.R., and Stolper, E.M., 1997, Oxygen isotope variations in ocean island basalt phenocrysts: Geochimica et Cosmochimica Acta, v. 61, p. 2281–2293, https://doi.org/10.1016/S0016-7037(97)00075-6.

Eiler, J.M., Farley, K.A., Valley, J.W., Stolper, E.M., Hauri, E.H., and Craig, H., 1995, Oxygen isotope evidence against bulk recycled sediment in the mantle sources of Pitcairn Island lavas: Nature 1995 377:6545, v. 377, p. 138–141, https://doi.org/10.1038/377138a0.

Eisele, J., Sharma, M., Galer, S.J.G., Blichert-Toft, J., Devey, C.W., and Hofmann, A.W., 2002, The role of sediment recycling in EM-1 inferred from Os, Pb, Hf, Nd, Sr isotope and trace element systematics of the Pitcairn hotspot: Earth and Planetary Science Letters, v. 196, p. 197–212, https://doi.org/10.1016/S0012-821X(01)00601-X.

Evans, K.A., 2012, The redox budget of subduction zones: Earth-Science Reviews, v. 113, p. 11–32, https://doi.org/10.1016/J.EARSCIREV.2012.03.003.

French, S.W., and Romanowicz, B., 2015, Broad plumes rooted at the base of the Earth's mantle beneath major hotspots: Nature 2015 525:7567, v. 525, p. 95–99, https://doi.org/10.1038/nature14876.

Freymuth, H., Vils, F., Willbold, M., Taylor, R.N., and Elliott, T., 2015, Molybdenum mobility and isotopic fractionation during subduction at the Mariana arc: Earth and Planetary Science Letters, v. 432, p. 176–186, https://doi.org/10.1016/j.epsl.2015.10.006.

Freymuth, H., Elliott, T., van Soest, M., and Skora, S., 2016, Tracing subducted black shales in the Lesser Antilles arc using molybdenum isotope ratios: Geology, v. 44, p. 987–990, doi:10.1130/G38344.1.

Gale, A., Dalton, C.A., Langmuir, C.H., Su, Y., and Schilling, J.G., 2013, The mean composition of ocean ridge basalts: Geochemistry, Geophysics, Geosystems, v. 14, p. 489–518, https://doi.org/10.1029/2012GC004334.

Garapić, G., Jackson, M.G., Hauri, E.H., Hart, S.R., Farley, K.A., Blusztajn, J.S., and Woodhead, J.D., 2015, A radiogenic isotopic (He-Sr-Nd-Pb-Os) study of lavas from the Pitcairn hotspot: Implications for the origin of EM-1 (enriched mantle 1): Lithos, v. 228–229, p. 1–11, https://doi.org/10.1016/J.LITHOS.2015.04.010.

Gaschnig, R.M., Rader, S.T., Reinhard, C.T., Owens, J.D., Planavsky, N., Wang, X., Asael, D., Greaney, A., and Helz, R., 2021a, Behavior of the Mo, Tl, and U isotope systems during

differentiation in the Kilauea Iki lava lake: Chemical Geology, v. 574, p. 120239, https://doi.org/10.1016/J.CHEMGEO.2021.120239.

Gaschnig, R.M., Reinhard, C.T., Planavsky, N.J., Wang, X., Asael, D., and Chauvel, C., 2017, The molybdenum isotope system as a tracer of slab input in subduction zones: An example from Martinique, Lesser Antilles Arc: Geochemistry, Geophysics, Geosystems, v. 18, p. 4674–4689, https://doi.org/10.1002/2017GC007085.

Gaschnig, R.M., Reinhard, C.T., Planavsky, N.J., Wang, X., Asael, D., and Jackson, M.G., 2021b, The impact of primary processes and secondary alteration on the stable isotope composition of ocean island basalts: Chemical Geology, v. 581, p. 120416, doi:10.1016/J.CHEMGEO.2021.120416.

Goldberg, T., Gordon, G., Izon, G., Archer, C., Pearce, C.R., McManus, J., Anbar, A.D., and Rehkämper, M., 2013, Resolution of inter-laboratory discrepancies in Mo isotope data: An intercalibration: Journal of Analytical Atomic Spectrometry, v. 28, p. 724–735, https://doi.org/10.1039/c3ja30375f.

Greber, N.D., Pettke, T., and Nägler, T.F., 2014, Magmatic–hydrothermal molybdenum isotope fractionation and its relevance to the igneous crustal signature: Lithos, v. 190–191, p. 104–110, doi:10.1016/J.LITHOS.2013.11.006.

Greber, N.D., Siebert, C., Nägler, T.F., and Pettke, T., 2012, $\delta^{98/95}$Mo values and molybdenum concentration data for NIST SRM 610, 612 and 3134: Towards a common protocol for reporting Mo data: Geostandards and Geoanalytical Research, v. 36, p. 291–300, https://doi.org/10.1111/j.1751-908X.2012.00160.x.

Hekinian, R. et al., 2003, The Pitcairn hotspot in the South Pacific: distribution and composition of submarine volcanic sequences: Journal of Volcanology and Geothermal Research, v. 121, p. 219–245, https://doi.org/10.1016/S0377-0273(02)00427-4.

Hin, R.C., Hibbert, K.E.J., Chen, S., Willbold, M., Andersen, M.B., Kiseeva, E.S., Wood, B.J., Niu, Y., Sims, K.W.W., and Elliott, T., 2022, The influence of crustal recycling on the molybdenum isotope composition of the Earth's mantle: Earth and Planetary Science Letters, v. 595, p. 117760, https://doi.org/10.1016/J.EPSL.2022.117760.

Honda, M., and Woodhead, J.D., 2005, A primordial solar-neon enriched component in the source of EM-I-type ocean island basalts from the Pitcairn Seamounts, Polynesia: Earth and Planetary Science Letters, v. 236, p. 597–612, https://doi.org/10.1016/J.EPSL.2005.05.038.

Jackson, M.G., Becker, T.W., and Konter, J.G., 2018, Geochemistry and distribution of recycled domains in the mantle inferred from Nd and Pb isotopes in oceanic hot spots: Implications for storage in the large low shear wave velocity provinces: Geochemistry, Geophysics, Geosystems, v. 19, p. 3496–3519, https://doi.org/10.1029/2018GC007552.

Jackson, M.G., Becker, T.W., and Steinberger, B., 2021, Spatial characteristics of recycled and primordial reservoirs in the deep mantle: Geochemistry, Geophysics, Geosystems, v. 22, p. e2020GC009525, https://doi.org/10.1029/2020GC009525.

Jones, T.D., Maguire, R.R., van Keken, P.E., Ritsema, J., Koelemeijer, P., 2020, Subducted oceanic crust as the origin of seismically slow lower-mantle structures. Progress in Earth and Planetary Science, v. 7, p. 17. https://doi.org/10.1186/s40645-020-00327-1.

Kaufmann, A.K.C., Pettke, T., and Wille, M., 2021, Molybdenum isotope fractionation at upper-crustal magmatic-hydrothermal conditions: Chemical Geology, v. 578, p. 120319, https://doi.org/10.1016/J.CHEMGEO.2021.120319.

Keller, C.B., and Schoene, B., 2012, Statistical geochemistry reveals disruption in secular lithospheric evolution about 2.5 Gyr ago: Nature, v. 485, p. 490–493, https://doi.org/10.1038/nature11024.

Kendall, B., Dahl, T.W., and Anbar, A.D., 2017, Good Golly, Why Moly? The stable isotope geochemistry of molybdenum, in: Non-Traditional Stable Isotopes, Walter de Gruyter GmbH, v. 82, p. 683–732, https://doi.org/10.2138/rmg.2017.82.16.

König, S., Wille, M., Voegelin, A., and Schoenberg, R., 2016, Molybdenum isotope systematics in subduction zones: Earth and Planetary Science Letters, v. 447, p. 95–102, https://doi.org/10.1016/j.epsl.2016.04.033.

Kump, L.R., and Barley, M.E., 2007, Increased subaerial volcanism and the rise of atmospheric oxygen 2.5 billion years ago: Nature 2007 448:7157, v. 448, p. 1033–1036, https://doi.org/10.1038/nature06058.

Laakso, T.A., and Schrag, D.P., 2019, A small marine biosphere in the Proterozoic: Geobiology, v. 17, p. 161–171, https://doi.org/10.1111/GBI.12323.

Labidi, J., Cartigny, P., Hamelin, C., Moreira, M., Dosso, L., 2014. Sulfur isotope budget (32S, 33S, 34S and 36S) in Pacific–Antarctic ridge basalts: A record of mantle source heterogeneity and hydrothermal sulfide assimilation. Geochimica et Cosmochimica Acta v. 133, p. 47–67. https://doi.org/10.1016/J.GCA.2014.02.023.

Labidi, J., Cartigny, P., and Moreira, M., 2013, Non-chondritic sulphur isotope composition of the terrestrial mantle: Nature 2013 501:7466, v. 501, p. 208–211, https://doi.org/10.1038/nature12490.

Labidi, J., Dottin, J.W., Clog, M., Hemond, C., and Cartigny, P., 2022, Near-zero 33S and 36S anomalies in Pitcairn basalts suggest Proterozoic sediments in the EM-1 mantle plume: Earth and Planetary Science Letters, v. 584, p. 117422, https://doi.org/10.1016/J.EPSL.2022.117422.

Lee, C.-T.A., Yeung, L.Y., McKenzie, N.R., Yokoyama, Y., Ozaki, K., and Lenardic, A., 2016, Two-step rise of atmospheric oxygen linked to the growth of continents: Nature Geoscience, v. 9, p. 417–424, https://doi.org/10.1038/ngeo2707.

Li, Z.X., Mitchell, R.N., Spencer, C.J., Ernst, R., Pisarevsky, S., Kirscher, U., and Murphy, J.B., 2019, Decoding Earth's rhythms: Modulation of supercontinent cycles by longer superocean episodes: Precambrian Research, v. 323, p. 1–5, https://doi.org/10.1016/j.precamres.2019.01.009.

Liang, Y.H., Halliday, A.N., Siebert, C., Fitton, J.G., Burton, K.W., Wang, K.L., and Harvey, J., 2017, Molybdenum isotope fractionation in the mantle: Geochimica et Cosmochimica Acta, v. 199, p. 91–111, https://doi.org/10.1016/j.gca.2016.11.023.

Liu, H., Zartman, R.E., Ireland, T.R., and Sun, W. dong, 2019, Global atmospheric oxygen variations recorded by Th/U systematics of igneous rocks: Proceedings of the National Academy of Sciences of the United States of America, v. 116, p. 18854–18859, https://doi.org/10.1073/pnas.1902833116.

Lyons, T.W., Reinhard, C.T., and Planavsky, N.J., 2014, The rise of oxygen in Earth's early ocean and atmosphere: Nature 2014 506:7488, v. 506, p. 307–315, https://doi.org/10.1038/nature13068.

Ma, L., Xu, Y.G., Li, J., Chen, L.H., Liu, J.Q., Li, H.Y., Huang, X.L., Ma, Q., Hong, L.B., and Wang, Y., 2022, Molybdenum isotopic constraints on the origin of EM1-type continental intraplate basalts: Geochimica et Cosmochimica Acta, v. 317, p. 255–268, https://doi.org/10.1016/J.GCA.2021.11.013.

McCoy-West, A.J., Chowdhury, P., Burton, K.W., Sossi, P., Nowell, G.M., Fitton, J.G., Kerr, A.C., Cawood, P.A., and Williams, H.M., 2019, Extensive crustal extraction in Earth's early history inferred from molybdenum isotopes: Nature Geoscience, v. 12, p. 946–951, https://doi.org/10.1038/s41561-019-0451-2.

Michael, P.J., and Cornell, W.C., 1998, Influence of spreading rate and magma supply on crystallization and assimilation beneath mid-ocean ridges: Evidence from chlorine and major element chemistry of mid-ocean ridge basalts: Journal of Geophysical Research: Solid Earth, v. 103, p. 18325–18356, https://doi.org/10.1029/98JB00791.

Nebel-Jacobsen, Y., Wille, M., Ivanic, T., and Nebel, O., 2021, Molybdenum isotope systematics in cumulate rock of the 2.8 Windimurra layered intrusion: A test for igneous differentiation and the composition of the Archean mantle: Precambrian Research, v. 355, p. 106087, https://doi.org/10.1016/J.PRECAMRES.2020.106087.

Newsom, H.E., White, W.M., Jochum, K.P., and Hofmann, A.W., 1986, Siderophile and chalcophile element abundances in oceanic basalts, Pb isotope evolution and growth of the Earth's core: Earth and Planetary Science Letters, v. 80, p. 299–313, https://doi.org/10.1016/0012-821X(86)90112-3.

Niu, Y., 2018. Origin of the LLSVPs at the base of the mantle is a consequence of plate tectonics – A petrological and geochemical perspective. Geoscience Frontiers, SPECIAL ISSUE: Frontiers in geoscience: A tribute to Prof. Xuanxue Mo, v. 9, p. 1265–1278. https://doi.org/10.1016/j.gsf.2018.03.005.

O'Sullivan, E.M., Nägler, T.F., Babechuk, M.G., 2021. Unusually heavy stable Mo isotope signatures of the Ottawa River: Causes and implications for global riverine Mo fluxes. Chemical Geology v. 568, p. 120039. https://doi.org/10.1016/j.chemgeo.2020.120039.

Padrón-Navarta, J.A., López Sánchez-Vizcaíno, V., Menzel, M.D., Gómez-Pugnaire, M.T., and Garrido, C.J., 2023, Mantle wedge oxidation from deserpentinization modulated by sediment-

derived fluids: Nature Geoscience 2023 16:3, v. 16, p. 268–275, doi:10.1038/s41561-023-01127-0.

Patchett, P.J., White, W.M., Feldmann, H., Kielinczuk, S., Hofmann, A.W., 1984. Hafnium/rare earth element fractionation in the sedimentary system and crustal recycling into the Earth's mantle. Earth and Planetary Science Letters v. 69, p. 365–378. https://doi.org/10.1016/0012-821X(84)90195-X.

Plank, T., and Langmuir, C.H., 1998, The chemical composition of subducting sediment and its consequences for the crust and mantle: Chemical Geology, v. 145, p. 325–394, https://doi.org/10.1016/S0009-2541(97)00150-2.

Putirka, K., 2008, Excess temperatures at ocean islands: Implications for mantle layering and convection: Geology, v. 36, p. 283–286, https://doi.org/10.1130/G24615A.1.

le Roux, P.J., Le Roex, A.P., Schilling, J.G., Shimizu, N., Perkins, W.W., and Pearce, N.J.G., 2002, Mantle heterogeneity beneath the southern Mid-Atlantic Ridge: trace element evidence for contamination of ambient asthenospheric mantle: Earth and Planetary Science Letters, v. 203, p. 479–498, https://doi.org/10.1016/S0012-821X(02)00832-4.

Siebert, C., Nägler, T.F., and Kramers, J.D., 2001, Determination of molybdenum isotope fractionation by double-spike multicollector inductively coupled plasma mass spectrometry: Geochemistry, Geophysics, Geosystems, v. 2, https://doi.org/10.1029/2000GC000124.

Skora, S., Freymuth, H., Blundy, J., Elliott, T., and Guillong, M., 2017, An experimental study of the behaviour of cerium/molybdenum ratios during subduction: Implications for tracing the slab component in the Lesser Antilles and Mariana Arc: Geochimica et Cosmochimica Acta, v. 212, p. 133–155, https://doi.org/10.1016/j.gca.2017.05.025.

Smit, M.A., and Mezger, K., 2017, Earth's early O_2 cycle suppressed by primitive continents: Nature Geoscience, v. 10, p. 788–792, doi:10.1038/ngeo3030.

Sperling, E.A., Wolock, C.J., Morgan, A.S., Gill, B.C., Kunzmann, M., Halverson, G.P., Macdonald, F.A., Knoll, A.H., Johnston, D.T., 2015. Statistical analysis of iron geochemical data suggests limited late Proterozoic oxygenation. Nature 2015 523:7561 v. 523, p. 451–454. https://doi.org/10.1038/nature14589.

Stolper, D.A., and Bucholz, C.E., 2019, Neoproterozoic to early Phanerozoic rise in island arc redox state due to deep ocean oxygenation and increased marine sulfate levels: Proceedings of the National Academy of Sciences of the United States of America, v. 116, p. 8746–8755, https://doi.org/10.1073/pnas.1821847116.

Storck, J.C., Greber, N.D., Duarte, J.F.V., Lanari, P., Tiepolo, M., and Pettke, T., 2023, Molybdenum and titanium isotopic signatures of arc-derived cumulates: Chemical Geology, v. 617, p. 121260, doi:10.1016/J.CHEMGEO.2022.121260.

Stracke, A., 2012, Earth's heterogeneous mantle: A product of convection-driven interaction between crust and mantle: Chemical Geology, v. 330–331, p. 274–299, https://doi.org/10.1016/J.CHEMGEO.2012.08.007.

Thoby, M., Konhauser, K.O., Fralick, P.W., Altermann, W., Visscher, P.T., and Lalonde, S. V., 2019, Global importance of oxic molybdenum sinks prior to 2.6 Ga revealed by the Mo isotope composition of Precambrian carbonates: Geology, v. 47, p. 559–562, doi:10.1130/G45706.1.

Villalobos-Orchard, J., Freymuth, H., O'Driscoll, B., Elliott, T., Williams, H., Casalini, M., Willbold, M., 2020. Molybdenum isotope ratios in Izu arc basalts: The control of subduction zone fluids on compositional variations in arc volcanic systems. Geochimica et Cosmochimica Acta, v. 288, p. 68–82. https://doi.org/10.1016/j.gca.2020.07.043.Voegelin, A.R., Nägler, T.F., Samankassou, E., and Villa, I.M., 2009, Molybdenum isotopic composition of modern and Carboniferous carbonates: Chemical Geology, v. 265, p. 488–498, https://doi.org/10.1016/j.chemgeo.2009.05.015.

Voegelin, A. R., Nägler, T. F., Beukes, N. J., and Lacassie, J. P. (2010). Molybdenum isotopes in late Archean carbonate rocks: Implications for early Earth oxygenation: Precambrian Research, v. 182(1–2), p. 70–82. https://doi.org/10.1016/j.precamres.2010.07.001.

Voegelin, A.R., Pettke, T., Greber, N.D., von Niederhäusern, B., and Nägler, T.F., 2014, Magma differentiation fractionates Mo isotope ratios: Evidence from the Kos Plateau Tuff (Aegean Arc): Lithos, v. 190–191, p. 440–448, https://doi.org/10.1016/j.lithos.2013.12.016.

Wang, W., Xu, Y., Sun, D., Ni, S., Wentzcovitch, R., Wu, Z., 2020, Velocity and density characteristics of subducted oceanic crust and the origin of lower-mantle heterogeneities. Nature Communications v. 11, p. 64. https://doi.org/10.1038/s41467-019-13720-2.

Wang, X.J. et al., 2018, Recycled ancient ghost carbonate in the Pitcairn mantle plume: Proceedings of the National Academy of Sciences of the United States of America, v. 115, p. 8682–8687, https://doi.org/10.1073/pnas.1719570115.

Willbold, M., and Elliott, T., 2017, Molybdenum isotope variations in magmatic rocks: Chemical Geology, v. 449, p. 253–268, https://doi.org/10.1016/j.chemgeo.2016.12.011.

Willbold, M., and Stracke, A., 2006, Trace element composition of mantle end-members: Implications for recycling of oceanic and upper and lower continental crust: Geochemistry, Geophysics, Geosystems, v. 7, https://doi.org/10.1029/2005GC001005.

Willbold, M., Hibbert, K., Lai, Y.-J., Freymuth, H., Hin, R.C., Coath, C., Vils, F., and Elliott, T., 2016, High-precision mass-dependent molybdenum isotope variations in magmatic rocks determined by double-spike MC-ICP-MS: Geostandards and Geoanalytical Research, v. 40, p. 389–403, https://doi.org/10.1111/j.1751-908X.2015.00388.x.

Wille, M., Nebel, O., Van Kranendonk, M.J., Schoenberg, R., Kleinhanns, I.C., and Ellwood, M.J., 2013, Mo-Cr isotope evidence for a reducing Archean atmosphere in 3.46-2.76Ga black shales from the Pilbara, Western Australia: Chemical Geology, v. 340, p. 68–76, https://doi.org/10.1016/j.chemgeo.2012.12.018.

Wille, M., Nebel, O., Pettke, T., Vroon, P.Z., König, S., and Schoenberg, R., 2018, Molybdenum isotope variations in calc-alkaline lavas from the Banda arc, Indonesia: Assessing the effect of crystal fractionation in creating isotopically heavy continental crust: Chemical Geology, v. 485, p. 1–13, https://doi.org/10.1016/j.chemgeo.2018.02.037.

Woodhead, J., and McCulloch, M., 1989, Ancient seafloor signals in Pitcairn Island lavas and evidence for large amplitude, small length-scale mantle heterogeneities: Earth and Planetary Science Letters, v. 94, p. 257–273, https://doi.org/10.1016/0012-821X(89)90145-3.

Yang, J., Siebert, C., Barling, J., Savage, P., Liang, Y.H., and Halliday, A.N., 2015, Absence of molybdenum isotope fractionation during magmatic differentiation at Hekla volcano, Iceland: Geochimica et Cosmochimica Acta, v. 162, p. 126–136, https://doi.org/10.1016/j.gca.2015.04.011.

Yierpan, A., König, S., Labidi, J., and Schoenberg, R., 2020, Recycled selenium in hot spot–influenced lavas records ocean-atmosphere oxygenation: Science Advances, v. 6, p. eabb6179, https://doi.org/10.1126/SCIADV.ABB6179.

Zerkle, A.L., 2018, Biogeodynamics: bridging the gap between surface and deep Earth processes: Philosophical Transactions of the Royal Society A: Mathematical, Physical and Engineering Sciences, v. 376, https://doi.org/10.1098/RSTA.2017.0401.

Zhao, P.-P., Li, J., Zhang, L., Wang, Z.-B., Kong, D.-X., Ma, J.-L., Wei, G.-J., and Xu, J.-F., 2016, Molybdenum mass fractions and isotopic compositions of International Geological Reference Materials: Geostandards and Geoanalytical Research, v. 40, p. 217–226, https://doi.org/10.1111/j.1751-908X.2015.00373.x.